Adsorption (2019) 25:923–936
https://doi.org/10.1007/s10450-019-00117-2

Properties of the Langmuir and Langmuir–Blodgett monolayers of cholesterol-cyclosporine A on water and polymer support

K. Przykaza[1] · K. Woźniak[1] · M. Jurak[1] · A. E. Wiącek[1] · R. Mroczka[2]

Received: 3 December 2018 / Revised: 7 May 2019 / Accepted: 10 May 2019 / Published online: 27 May 2019

Abstract
The paper deals with the cholesterol–cyclosporine A (Chol–CsA) monolayers at the air/water interface investigated using the Langmuir trough coupled with the Brewster's angle microscopy. The compressed films were transferred onto the PEEK polymer support by means of the Langmuir–Blodgett technique. To improve molecules adhesion and organization the PEEK surface was treated with air plasma before thin films deposition. The obtained surfaces were characterized by means of atomic force microscope (AFM). Then, the wettability of the supported monolayers was determined by the contact angle measurements. Finally, the surface free energy and its components were evaluated from the theoretical approach proposed by van Oss et al. The obtained results reveal correlation between properties of the Langmuir monolayers at the air/water interface and those of the Langmuir–Blodgett films on PEEK. This was found to be helpful for understanding the wettability of organized molecular films on the polymer support as far as biocompatibility improve is concerned. The preparation of films with defined polarity and various compositions is an important step in the development of polymer surfaces with increased biofunctionality. It is believed that the results presented in this paper can be exploited in the in vivo studies.

Keywords Langmuir monolayer · Cyclosporine A · Cholesterol · Polyetheretherketone · Atomic force microscopy · Wettability · Surface free energy

1 Introduction

Both natural and synthetic polymers are common in our environment. Owing to their properties they find many applications in various areas of life, e.g. they can be used in textile, building and food industry as well as in medicine (Hubbell 1994). The group of polymers with phenomenal mechanical and dielectric properties such as great mechanical and chemical resistance, thermal and radiation stability and biocompatibility to living tissues includes polyaryletherketones (PAEKs). The main representative polymer of this group is polyetheretherketone (PEEK). PEEK is a semi-crystalline linear polycyclic aromatic thermoplastic (Fig. 1). It has an aromatic molecular backbone with functional groups between the aryl rings (Kurtz 2012; Ma and Tang 2014; Wiącek et al. 2016a, b).

Polymers, such as PEEK used in medicine for making prostheses or implants (orthopedic, traumatic or spinal) must have some important attributes, such as biocompatibility and non-toxicity. Biocompatibility means ability to induce an acceptable response of the body. Biocompatible polymers are those that themselves and products of their degradation do not cause allergies (Rui et al. 2014; Frederik et al. 2015; Najeeb et al. 2016; Lvhua et al. 2017; Ryan and Getgood 2017). To improve biocompatibility scientists modify the polymer surface by biological, physical, chemical or mixed methods. In the first method the biologically active substances are immobilized on the polymer surface. Owing to this operation biocompatibility is much better. The physical methods include: flame modification, laser, electron or ion beam as well as hot or cold plasma treatment. Plasma is an electric inert ionized gas with a large amount of particles.

This article belongs to S.I. ISSHAC10, but it reach the press at the time the special issue was published.

✉ K. Przykaza
przykaza.kacper@poczta.umcs.lublin.pl

[1] Department of Physical Chemistry-Interfacial Phenomena, Faculty of Chemistry, University of Maria Curie-Skłodowska, Maria Curie-Skłodowska Sq. 3, 20-031 Lublin, Poland

[2] Laboratory of X-ray Optics, Centre for Interdisciplinary Research, The John Paul II Catholic University of Lublin, Konstantynów 1J, 20-708 Lublin, Poland

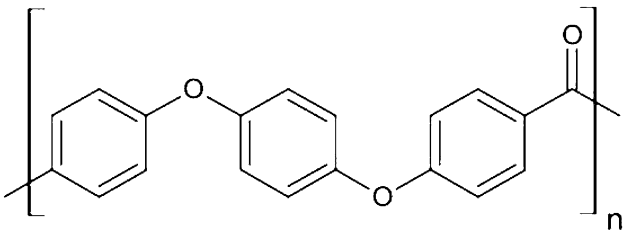

Fig. 1 Structure of polyetheretherketone (PEEK)

It consists mainly of atoms, metastable molecules, positive and negative ions, electrons, photons and radicals. Chemical methods deal with chemical reactions between atoms or molecules of polymer and other substances. Chemical reactions or creation of an additional outer layer on the support surface are a result of surface etching and/or deposition of thin films of biologically active substances, for example using a Langmuir–Blodgett trough. During polymer surface modification for medical use, there is a risk of introducing additional impurities. To avoid them, especially in the aspect of potential biomedical applications, activities that can prevent such phenomena should be applied (Garbassi et al. 1994; Favia and d'Agostino 1998; Gan et al. 2016). The use of low-temperature plasma, which thoroughly cleans the polymer surface can minimize this process (Dannes and Schwartz 2009; Novotna et al. 2015; Ma and Tang 2014; Botel et al. 2018). Due to the high chemical and biological inertness of the PEEK surface, the process of osteointegration is inadequate and slow. In order to improve this limitation, the use of physical (cold plasma) and chemical (biocoating) modifications seems to be the proper trend of modification and testing this type of surface. The similarly targeted studies were recently published by Mahjoubi et al. (2017) and Fukuda et al. (2019).

Additionally, there is possibility to immobilize biologically active substances onto the PEEK surface, such as immunosuppressants, antibiotics or even growth factors (Kantlehner et al. 2000). This process can improve preventing from implant rejection by the human body and accelerate convalescence. One of these substances is cyclosporine A (CsA) (Fig. 2a), cyclic polypeptide. CsA has been known for a long time. It was discovered in 1971 as a substance produced by fungus *Tolypocladium inflatum.* CsA is used to prevent the transplant of the organ such as heart, kidneys, liver, pancreas or lungs from rejection and to treat psoriasis, rheumatoid arthritis or dry eye disease. Owing to its profound hydrophobicity and cyclic structure it can interact with many molecules, especially with those building cell membranes in human cells (brain, nerve cells) (Bundgaard and Friis 1992). Some studies indicate that CsA can change membrane organization. It abolishes the pretransition for saturated phospholipids which leads to decrease in their main transition temperature and enthalpy (O'Learyl et al. 1986; Wiedman et al. 1990). The other studies suggest that CsA can increase or decrease the lamellar-to-hexagonal phase transition temperature of phospholipids depending on its molar ratio, or even inhibit fusion of the biological membranes (Epand et al. 1987). Investigations of the interactions of CsA with the biological membranes can be specified by examining its interactions with individual components such as cholesterol (Fig. 2b). This lipid plays a very important role in maintaining the stiffness of the membrane and determines its permeability to other substances (Loosli et al. 1985; Ohvo-Rekilä et al. 2002; Costa et al. 2012). It should be taken into account that Chol is also a main component of the rafts which are currently hot-topic in science (Leslie 2011). CsA has preference for energetically favorable fluid/gel domain bonds (Weis and McConell 1985). Soderlund et al. (1999) investigated the influence of CsA on various phospholipid-cholesterol thin films by differential scanning calorimetry and fluorescence microscopy. They observed rapid binding of CsA to the lipid monolayers. Accordingly, the simultaneous use of Chol and CsA can improve the PEEK surface biocompatibility, enhance coatings stability and finally prevent the rejection (Hawskhaw et al. 2018).

Since the polymer support coatings are getting more attended nowadays, these studies were aimed at modifying the air plasma activated PEEK surface by deposition of the biologically active monolayers. The recently published

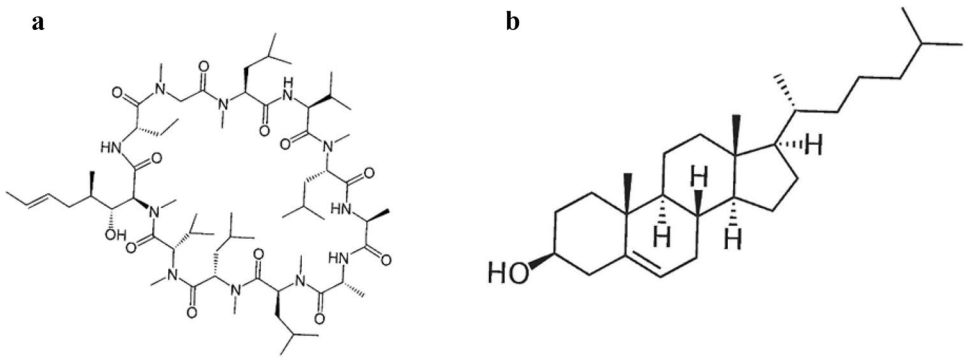

Fig. 2 Structure of cyclosporine A—CsA (**a**) and cholesterol—Chol (**b**)

papers on the PEEK air plasma activation prove that such a process leads to the formation of new polar functional groups on the polymer surface, thus increasing its surface free energy and adhesion (Comyn et al. 1996; Zhang et al. 2011; Bhatnagar et al. 2012; Terpiłowski et al. 2018). This facilitates adsorption of the biological molecules onto the polymer support to obtain the surface of defined polarity as well as the increased biocompatibility.

The main goal of this paper was to characterize properties of the Chol–CsA monolayers at the air/water interface in terms of their organization and packing as well as possibility to transfer the obtained thin films onto the activated polymer support. In order to estimate behaviour of the Chol–CsA mixed system at the air/water interface the Langmuir trough coupled with the Brewster's angle microscopy has been applied. Based on the π-A isotherms, monolayer morphology and thickness, properties of the systems with different Chol:CsA molar fractions ($X_{CsA} = 0.25$; 0.5 and 0.75) were characterized. Then, the obtained monolayers were transferred onto polyetheretherketone (PEEK) using the Langmuir–Blodgett technique at the surface pressure of 15 mN/m or 30 mN/m (only Chol). To enhance molecules adhesion, the polymeric surfaces were activated for 1 min with the low temperature and low pressure air plasma before thin films deposition. The prepared modified PEEK surfaces have been subjected to wettability measurements using the system of three liquids with different polarity (water, formamide, diiodomethane) as well as structure determination by means of atomic force microscopy. Moreover, the topography analysis by optical profilometry was conducted and presented in our other paper (Przykaza et al. 2019). On the basis of contact angles measurements the values of apparent surface free energy and its components were estimated using the van Oss et al. approach (1989; 1990). Some correlations between physicochemical properties of the monolayers before and after transfer onto the polymer support were found. Moreover, the studies allowed to estimate polarity of the PEEK surface (unmodified, modified with plasma and/or Chol–CsA monolayers) which is very important in the case of proper in vivo studies as well as in projecting and planning polymer coatings used in many branches of science.

2 Materials and methods

2.1 Registration of π-A isotherms, BAM images and relative thickness of layer

Appropriate amounts of cholesterol (Chol) and cyclosporine A (CsA) were dissolved in the chloroform–methanol solution, 4:1 v/v (solvents from Avantor Performance Materials Poland S.A) to obtain the final concentration of 1 mg/mL, right before spreading onto water subphase. Chol was purchased from Sigma-Aldrich and CsA from Alfa Aesar, both with the purity above 99%. Mixtures containing different molar ratios of CsA ($X_{CsA} = 0.15$; 0.25; 0.5 and 0.75) were prepared by mixing suitable volumes of pure solutions. During the tests the first step was precise preparation of the Langmuir trough (KSV NIMA, Finland) – cleaning with methanol, filling with Milli-Q water (surface tension 72.8 mN/m), thermosetting to 20 °C and maintaining the surface pressure not to change more than 0.3 mN/m during the test-compression. After this procedure the proper amounts of previously prepared solutions were carefully spread onto the air/water interface using a microsyringe and left for 10 min for solvent evaporation. Then a thin layer of solution (applied film) was compressed with speed of 20 mm/min and the changes of surface pressure were registered by the Wilhelmy platinum plate. The computer software simultaneously calculated changes of area per molecule in the function of surface pressure rise and the π-A isotherm curve was registered.

At the same time the Brewster angle microscopy (BAM) was used to estimate the morphology of the obtained monolayers in function of their composition and surface pressure. BAM was also applied to examine the monolayers thickness based on the correlation between grey level and the relative reflectivity (Rodríguez Patino et al. 1999). Measurements of both parameters were performed in variant of a nanofilm_ultrabam (Accurion GmbH, Germany) equipped with a solid-state 50 mW laser emitting *p*-polarized light at 658 nm wavelength which was reflected off the air/water interface at the Brewster's angle equal to 53.2°. The size of the BAM images was $207 \times 192\ \mu m^2$.

For the layer thickness measurements, firstly BAM was calibrated to clear MilliQ water (if possible without any molecules at the interface) and the plot of grey level as a function of incidence angle was obtained. The minimum of the parabolic fit was the angle of incidence with the lowest reflectivity valid under the existing environmental conditions. After this step it was possible to convert the grey scale information into reflectivity. Then the single-layer optical model was applied to convert the reflectivity R into the film thickness d (Winsel et al. 2003) according to Eq. 1:

$$R = \frac{I_r}{I_0} = \left(\pi \frac{d}{\lambda}\right)^2 \frac{\left(n_1^2 - n_2^2 - 1 + \frac{n_2^2}{n_1^2}\right)^2}{1 + n_2^2} \tag{1}$$

where: I_0 and I_r are the incident and the reflected intensities, respectively; n_1 and n_2 denote the refractive indices of the film and the subphase, respectively; λ is the wavelength of the incident light.

2.2 Purification procedure of PEEK plates surface

PEEK plates (20 mm × 30 mm × 5 mm) were cut from the commercial TECAPEEK natural (size 1000 mm × 500 mm × 5 mm, PROFILEX) and purified to eliminate any surface contamination. Firstly, a solution of neutral extran (1 mL/100 mL of MilliQ water) was prepared and poured into a beaker with the PEEK plates which has been placed additionally in the ultrasonic bath. After that the plates were cleaned using methanol and finally 2–3 times with MilliQ water until its conductivity did not exceed 5 µS/cm. Each washing step improved by ultrasonic waves took 15 min. After the purification procedure the dried plates were put into a vacuum oven for 24 h.

2.3 Low-temperature plasma treatment of PEEK surface

Low temperature (20 °C) and low pressure (0.2 mbar) air plasma modification of PEEK surfaces procedure was conducted using the Pico plasma system (Diener Electronic, Germany). Similarly to our earlier studies (Wiącek et al. 2016a, b) PEEK plates were activated for 60 s with 460 W plasma with continuous air flow of 22 sccm (*standard cubic centimeters per minute*). Compared to the previous papers, the improved surface modification procedure was applied. In order to guarantee activation of both plate sides, special scaffolds were applied to keep the vertical position.

2.4 Deposition of Chol–CsA monolayers onto PEEK using the LB technique

For the precise deposition of organized thin films of Chol, CsA and their mixtures onto the plasma activated PEEK support the Langmuir trough (KSV 2000) equipped with the dip-arm system was applied. The procedure of the Langmuir trough cleaning before measurements and monolayer formation was the same as described in point 2.1. Just before spreading the bioactive molecules onto the water subphase, the plasma activated PEEK plates were attached to the dip arm and using the computer software placed deep under the sheet of water subphase in a special well of trough. The next step of studies included: molecules deposition onto the air/water subphase and the process of solvent evaporation (also described in point 2.1). When the surface pressure reached desired value (Table 1), the monolayer was stabilizing for 10 min and finally the dip-arm was moved up slowly while the transferring process started. During the whole process the barriers of Langmuir trough were kept at the constant value of transfer surface pressure. Experimental transferring parameters of compression speed and surface pressure during the transfer were correlated with the plots of π-A isotherms. The third parameter, transfer speed was experimentally selected. Using the transfer parameters presented in Table 1 the value of transfer ratio was revealed as close to one, which means that the obtained coating was a monolayer with high probability. After that the solid supported films were put into the Petri dishes and placed into the vacuum oven for 24 h. In case of cholesterol film for both transfer pressures of 15 mN/m and 30 mN/m the transfer ratio was found to be very close. The value of 15 mN/m was chosen based on the matching to the Chol–CsA mixed systems, for which it below the collapse pressure of the monolayer and the system is possibly the most packed and stable. The value of 30 mN/m corresponds to the lateral pressure of the biological membrane. Unfortunately this value is not possible to achieve in systems containing cyclosporine. Hence for further analysis Chol film deposited at surface pressure of 30 mN/m has been also chosen.

Table 1 Experimental transferring parameters

Substance(s)	Compression speed [mm/min]	Surface pressure during transfer [mN/m]	Transfer speed [mm/min]
Chol	20	15 and 30	5
CsA	20	15	5
Chol–CsA	20	15	5

2.5 Measurements using atomic force microscope

Roughness of the deposited layers as well as the PEEKair support was examined using an atomic force microscope (5600LS AFM, Agilent Technologies) in non-contact mode (tip radius < 2 nm, resonance frequency 280 kHz) with a resolution of 256 × 256 and scan area of 1 µm × 1 µm. The measurements were carried out at least in 12 different points. In the first place of sample (1) four points were selected in the distance 0.2 mm to each other. After measurements, sample was moved 2 mm to the second place (2) and four next points were selected in the same manner as for the first place. The third place on the surface was selected analogically as the places (1) and (2). The surface roughness, S_q,—the root mean square of arithmetic average of the surface roughness absolute values—was calculated using the Scanning Probe Image Processor (SPIP) v. 5.1.4 software (Image Metrology A/S, Denmark) according to the formula:

$$S_q = \sqrt{\frac{1}{MN}\sum_{k=0}^{M-1}\sum_{l=0}^{N-1}\left[z(x_k, y_l)\right]^2} \quad (2)$$

where: x and y are the coordinates, z is the perpendicular deviation from the ideally smooth surface, M is the number

of points in the x direction, and N is the number of points in the y direction.

2.6 Contact angle measurements of water, formamide and diiodomethane

The samples modified in accordance with the procedure discussed above were moved into the chamber of contact angle measuring system (DGD ADR model with GBX S.A.R.L) with constant flow of a nitrogen gas. For these experiments the system of three probe liquids, two polar: MilliQ water and formamide (Acrōs Organics, 99.5%) and one apolar diiodomethane (Aldrich, 99%) was chosen to determine values of advancing contact angles on the modified PEEK surfaces as well as to estimate values of surface free energy and its components. Each time the same amount of liquid, 6 µL was released using the microsyringe and the advancing contact angle was measured by the digital camera and the computer equipped with the WinDrop++software. For each system these measurements were conducted twice and minimum 12–16 droplets of each liquid were obtained. For the plasma activated PEEK surface the measurements were made after 10 min following the activation process. The values of average advancing contact angles of this triple probe liquid system were used for further surface free energy calculations.

2.7 Surface free energy (SFE) determination using the LWAB approach

In order to compare the tests carried out with our analogous measurements on the PEEK surface with other biological layer, SFE was calculated using the Van Oss et al. (1989; 1990) method (Lifshitz-van der Waals/acid–base).

This approach is based on the values of advancing contact angles of three liquids. Owing to application of two polar (water, formamide) and one apolar (diiodomethane) liquid, work of adhesion of every droplet can be divided into individual parts of complex interactions between the solid, liquid and air interfaces according to Eq. 3:

$$W_A = \gamma_l(1+\cos\theta) = 2\sqrt{\gamma_s^{LW}\gamma_l^{LW}} + 2\sqrt{\gamma_s^-\gamma_l^+} + 2\sqrt{\gamma_s^+\gamma_l^-} \quad (3)$$

where: W_A is the work of adhesion, γ_l is the liquid surface tension, θ is the advancing contact angle, $\gamma_{s/l}^{LW}$ are the solid or liquid apolar Lifshitz–van der Waals interactions, $\gamma_{s/l}^+$ is the electron-acceptor parameter for a solid or a liquid, and $\gamma_{s/l}^-$ are the electron-donor parameter for a solid or a liquid.

3 Results and discussion

3.1 Registered π-A isotherms

Figure 3 represents the π-A isotherms of mixed Chol–CsA monolayers. Cholesterol molecules form a stable monolayer on the water subphase at room temperature (20 °C). The π-A isotherm for Chol exhibits a rapidly growing course with a specific sharp shaped kink at the surface pressure of about 46 mN/m (Fig. 3). Cyclosporine A (CsA) also forms a stable monolayer at room temperature which collapses at about 24 mN/m. This is in agreement with the results of Malcolm et al. (1973), i.e. 26 mN/m. In this paper the authors also described behaviour of polypeptides packed films whose collapse pressure corresponded to an area of 17.5 Å^2 per amino acid residue. In our paper the area per CsA molecule at collapse was determined to be about 200 Å^2/molecule. As it has 11 amino acid residues theoretically the collapse area per molecule is 192.5 Å^2/molecule which is very close to the experimental one in our case.

After mixing those two compounds at the determined molar ratio (0.15, 0.25, 0.5 and 0.75) the differently shifted π-A isotherms were obtained strictly depending on the proportion of CsA and Chol. Thus the impact of CsA on the Chol film is indisputable. Even small addition of CsA to the Chol monolayers shifts their isotherms to that of pure CsA significantly (Fig. 3). All mixed isotherms exhibit the first collapse pressure at about $\pi_{coll} = 25$ mN/m. However, only in the proportion of $X_{CsA} = 0.15$ the second collapse π_{coll} was revealed characteristic of cholesterol at the surface pressure of 46 mN/m (Fig. 3). Generally, two collapses occur when components of the monolayer are immiscible. They

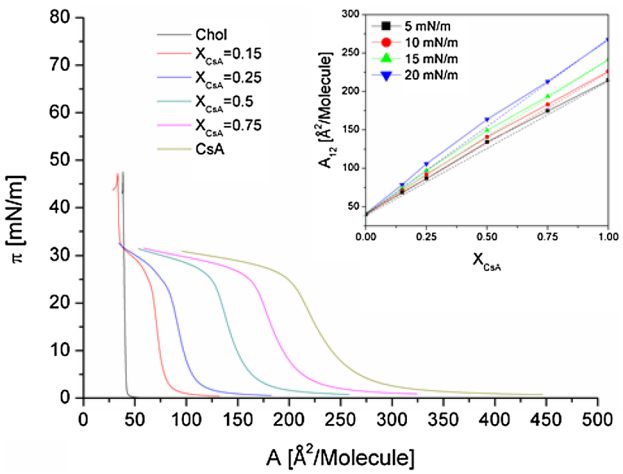

Fig. 3 Surface pressure-area (π–A) isotherms of the pure and mixed CsA-Chol monolayers registered on the water subphase at 20 °C and with 20 mm/min barrier compression. Inset: mean molecular area (A_{12})-X_{CsA} plots

correspond to the collapse surface pressures for the individual pure components. However, the component, whose monolayer collapses at lower surface pressure, is being squeezed out to the water subphase. Then the system remaining at the air–water interface is still the monolayer enriched in the second component, that collapses at the higher surface pressure (Gaines 1966; Dynarowicz-Łątka and Kita 1999; Jurak and Miñones 2013).

The other mixed monolayers did not expose the second collapse probably because of too low amounts of Chol molecules and/or limits of the Langmuir trough area (barriers touched the Wilhelmy's plate or could not compress to lesser areas). Moreover, for all mixed monolayers significant changes of mean molecular area per molecule are observed depending on the monolayer composition. As the amount of CsA increases, the mean molecular areas at each surface pressure gradually grow. Additionally as the surface pressure increases the mean molecular area values were observed to be shifted to higher values. The maximum of $A_{12}=215$ Å^2/molecule for $X_{CsA}=0.75$ was obtained at $\pi=5$ mN/m and the minimum of $A_{12}=68$ Å^2/molecule at $\pi=20$ mN/m for $X_{CsA}=0.15$. Moreover, at each value of surface pressure there was observed deviation from the linear course of A_{12} versus composition of the film. This can suggest that both components mix partially. The positive deviations from straightness can be associated with the occurrence of repulsive interactions between the two components of the mixture (Inset Fig. 3). The further analysis of miscibility based on the excess Gibbs energy is discussed in Sect. 3.3. Our results obtained from the π-A curves analysis are in agreement with those already published by the other authors (Dynarowicz-Łątka et al. 2015).

3.2 Compression modulus analysis

Based on a plot of the π-A curves, presented above it is possible to conclude about molecular behaviour of monolayer during compression. Davies and Rideal (1963) introduced the compressibility modulus (Cs^{-1}) (Eq. 4) to describe the behaviour of amphiphilic molecules at the air/water interface. Cs^{-1} allows to have better insight into the physical state (phase) and/or packing changes of molecules. In the next part of the paper Cs^{-1} was calculated and discussed.

$$Cs^{-1} = -A\left(\frac{d\pi}{dA}\right)_{T,n} \tag{4}$$

According to Davies and Rideal the liquid-expanded (LE) and liquid-condensed (LC) states are characterized by the Cs^{-1} values in the range of 12.5–50 mN/m and 100–250 mN/m, respectively. Moreover, the Cs^{-1} limit values for the solid state (LS) are 1000–2000 mN/m. For the pure Chol monolayer the Cs^{-1} parameter (Fig. 4) rapidly grows from 0 to 250 mN/m as the surface pressure increases from 0 to 3.3 mN/m. In this

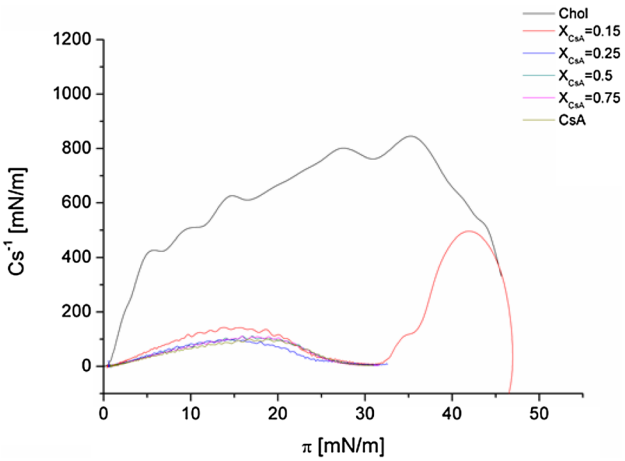

Fig. 4 Compressibility modulus Cs^{-1} of pure Chol, CsA monolayers and their mixtures with different molar ratios

range Chol reaches the LC state. Then, as the surface pressure grows the Cs^{-1} achieves high values up to 900 mN/m at $\pi=35.3$ mN/m, which can suggest that the Chol molecules remain in a tightly condensed state (LC) during compression (Cadena-Nava et al. 2006). Moreover, it is clearly visible that its film is more condensed at surface pressure of 30 mN/m ($Cs^{-1}=790$ mN/m) than at 15 mN/m ($Cs^{-1}=645$ mN/m) (Fig. 4).

The compressibility modulus values indicate the LE state for CsA. As presented in Fig. 4, $Cs^{-1}$of CsA constantly grows from the surface pressure of $\pi=2.7$ mN/m (322 Å^2/molecule) and then reaches the maximum at $\pi=14.9$ mN/m (243 Å^2/molecule). Moreover, CsA drastically decreases the Cs^{-1} values of Chol films, their packing and ordering (Fig. 4). After the addition of CsA to the Chol film, Cs^{-1}drops from about 500 mN/m to about 100 mN/m for each two-component film. This indicates the liquid-expanded state of the Chol–CsA monolayers. Similar observations were described by Wnętrzak et al. (2018) for the Chol-sphingomyelin mixed films. Moreover, CsA provokes formation of domain structure within the membrane with the coexisting LE/LC phases (see Sect. 3.4).

3.3 Excess functions

Directly from the π-A isotherm data, it was possible to estimate the qualitative and quantitative interactions as well as the behaviour between the molecules during the film compression (Gaines 1966). To evaluate interactions qualitatively the excess molecular area (A^{exc}) was needed. Then based on it, the changes of excess Gibbs energy (ΔG^{exc}) were calculated.

For the system, which consists of two components, A^{exc} is defined as:

$$A^{exc} = A_{1-2} - (A_1X_1 + A_2X_2) \tag{5}$$

where: A_{1-2} denotes the mean molecular area in the binary system, A_1 and A_2 are the molecular areas of components in the pure monolayers at the same surface pressure, X_1 and X_2 are the molar fractions of those components in the mixed monolayer.

The excess Gibbs energy changes are expressed as follows:

$$G^{exc} = N \int_0^{\pi} A^{exc} d\pi \tag{6}$$

where: N is the Avogadro's number and π means the surface pressure.

According to Gaines (1966) positive values of the ΔG^{exc} parameter suggest repulsive interactions between molecules at the air/water interface while negative ones can be an evidence for attractive interactions. Figure 5 presents the ΔG^{exc} values calculated for the CsA–Chol monolayers with the changing molar ratio of CsA at four different values of surface pressure before the collapse pressure (π_{coll}).

At each surface pressure the positive values of G^{exc} are observed similarly to those obtained by (Dynarowicz-Łątka et al. 2015). However, the maximum (1100 J/mol) appears at $X_{CsA} = 0.5$ at 20 mN/m while that reported by Dynarowicz-Łątka occurs at $X_{CsA} = 0.7$ (ca. 1750 J/mol) at the same surface pressure. The obtained discrepancy can be due to using CsA of different origin that can affect the strength of interactions. Based on the relationships presented in Fig. 5, it can be concluded that in the CsA–Chol mixed monolayers more repulsive interactions than in one-component systems occur (Fig. 5). CsA interacts strongly with the intermolecular H-bonds produced by the NH groups of amino acids (Abu-2, Ala-7,Val-5 and D-Ala-8) which determine its conformation at the air–water interface. Probably thereby CsA is weakly engaged in the interactions with Chol by this type of bonding.

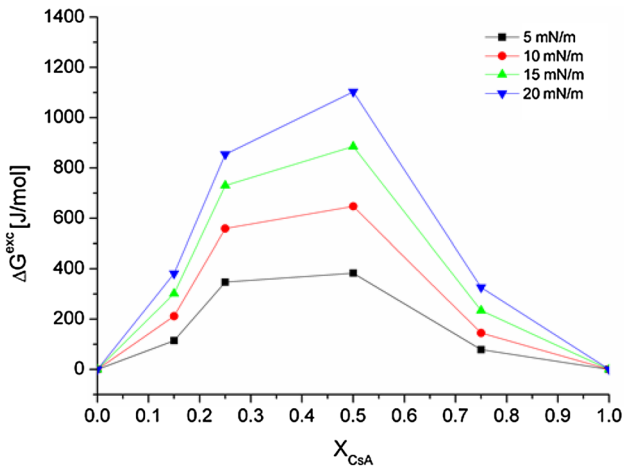

Fig. 5 Excess Gibbs energy of mixing (ΔG^{exc}) versus the mixed film composition (X_{CsA})

3.4 Morphology and thickness

Using the Brewster angle microscope (BAM) technique the morphology of pure cholesterol, CsA and their mixtures with the increasing molar ratio of CsA was observed. The images obtained at the surface pressure of 15 mN/m, the surface pressure of film transfer onto the polymer support, are shown in Fig. 6. In the case of monolayers consisting of one compound (Chol or CsA) a smooth and bright surface was visualized without any domains or aggregates up to the collapse. Cholesterol forms a stable and condensed monolayer starting from very low surface pressure values (3.3 mN/m). In addition morphology of the Chol monolayer at surface pressure of 15 mN/m and 30 mN/m is similar. The liquid condensed state of Chol proved Cs^{-1} high values up to about 900 mN/m (Fig. 4) and even very small additions of CsA cause a dramatic decrease of this parameter (Cs^{-1} = ~ 100 mN/m at $\pi = 15$ mN/m) changing the monolayer to liquid expanded/liquid-condensed state (Wnętrzak et al. 2018). This behaviour was also observed by Söderlund et al. (1999). Thus after the addition of CsA to Chol in various proportions there appear small irregular domains. This fact suggests partial miscibility of both components where the condensed Chol-rich domains coexist with the expanded CsA-rich domains. Such monolayers behaviour is confirmed by the positive values of excess Gibbs energy of mixing (Fig. 5) and it is in line with the other studies (Dynarowicz-Łątka et al. 2015).

Based on the reflectivity measurements obtained using the Brewster's angle microscopy (BAM) the relative thickness of the investigated monolayers was estimated by means of the single-layer optical model (Winsel et al. 2003). The results are presented in Fig. 7 depending on the stage of compression. As mentioned above the Chol and CsA monolayers are homogeneous (Fig. 6) irrespective of the surface pressure. The thickness of Chol film is practically constant (about 2.5 nm) in the whole range of surface pressure while that of CsA monolayer gradually increases with the pressure from 0.8 nm ($\pi = 5$ mN/m) to 1.52 nm (π_{coll}). The presence of CsA in the Chol monolayer causes the thickness decrease; the more the higher amount of CsA is used. At the surface pressure of 15 mN/m, that is the pressure of transfer onto the solid support, those films reach the thicknesses of 2.17; 1.91; 1.78; 1.46 nm at $X_{CsA} = 0.15$; 0.25; 0.5 and 0.75, respectively. For pure components at this surface pressure, the thickness was estimated to be 2.6 nm for Chol and 1.31 nm for CsA. As mentioned above the thickness of pure CsA is small during the whole compression, but gradually increases with the increasing molar fraction of

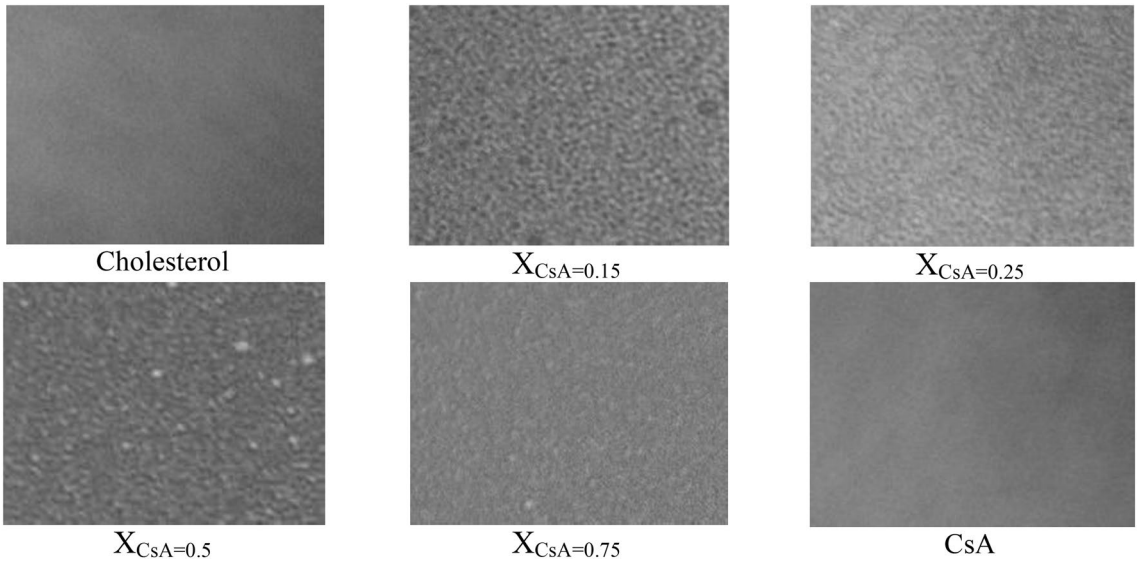

Fig. 6 BAM images registered at 15 mN/m on the water subphase for pure Chol, CsA and their mixtures with the molar fraction of CsA = 0.15; 0.25; 0.5 and 0.75. The presented area: 207 × 192 μm^2

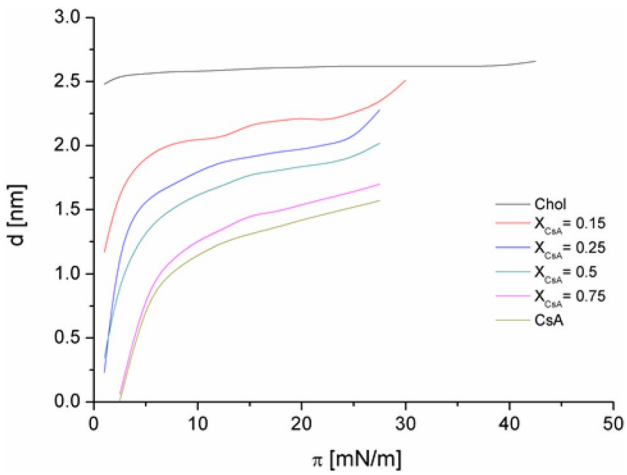

Fig. 7 Relative thickness of pure Chol, CsA and mixed Chol–CsA monolayers versus the surface pressure during compression

cholesterol. This can be explained by specific cholesterol-drug interactions reflected in the pressure-induced change in the conformation and/or orientation of CsA which can be very sensitive to Chol (Söderlund et al.1999). CsA alters dramatically the lateral organization in the obtained layers on a micrometer scale and, as postulated by the other authors (Schroeder et al.1995), the interactions of CsA with the biological membrane strongly depends on the Chol amount. Organization and orientation of Chol in the membranes, as proposed by Schroeder et al. (1995), can directly conduct their functions. A similar effect of Chol was described by Costa et al. (2012) where the Chol molecules deposited at the air/water interface allowed or not to incorporate the protein molecule into the monolayer depending on the type of acyl chain of adjacent phospholipids.

3.5 Surface topography

It is known from the literature that the Langmuir–Blodgett technique of transferring thin films from Langmuir trough onto the solid supports is very useful and appropriate for this kind of studies (Chen et al. 2007; Jurak et al. 2016; Jurak and Wiącek 2017). We believe that transfer of the compressed Langmuir monolayers onto the activated PEEK support by the LB technique maintains mostly their properties such as physical state, packing, ordering or domain structure, although the monomolecular coatings are not completely continuous due to high roughness of the PEEK. Moreover, the mutual interactions within the monolayers at the air/water interface, quantified by the changes of ΔG^{exc} can affect the deposition process, quality of the films, and finally their interactions with the probe liquids, thus wettability. Therefore the Langmuir monolayers of the Chol–CsA systems were transferred onto the plasma activated PEEK surface by the LB method at a surface pressure of 15 mN/m, with the exception of a cholesterol film for which transfer pressure was also 30 mN/m. This was confirmed, on the basis of the previously obtained isotherm curves, Cs^{-1} modulus and BAM images, that at the surface pressure of (15 mN/m) both components were present in the Chol–CsA monolayers, even though domains regularly distributed can be formed as a result of the repulsion forces. In the next stage, Chol–CsA monolayers of various composition were compressed to the given values of surface pressure and transferred onto the

activated PEEK surface. Its topography and surface roughness were studied using atomic force microscopy.

Distributions of the surface roughness defined by S_q parameter for seven samples: PEEKair, $Chol_{15mN/m}$, $Chol_{30mN/m}$, $X_{CsA}=0.25$; 0.5; 0.75 and CsA are shown in Fig. 8a–f. As it is clearly seen the surface roughness is highly deviated from a few nm (measured for all samples) up to 140 nm, only for $Chol_{30mN/m}$. The high values detected for $Chol_{30mN/m}$ is caused probably due to scanning within area that demonstrates high slope value. Taking into account that the standard deviation of surface roughness even for PEEKair is high, statistical description of the surface morphology in nanoscale is very uncertain and does not make sense. Due to this reason the most representative AFM micrographs for all studied samples that exhibited the lowest roughness were selected and are shown in Fig. 9. Based on them we tried to find morphological differences between samples to obtain their more qualitative description. The PEEKair surface as a support for Chol and CsA monolayers demonstrates characteristic of parallel ribbed structures with randomly distributed forms resembling crystallites. Surface roughness is rather moderate usually below 10 nm. The representative morphological features and the S_q value equal to 3.97 nm presented in Fig. 9a are typical for about 30% measured places on the PEEKair surface. This surface covered by $Chol_{15mN/m}$ is similar morphologically to PEEKair (Fig. 9a, b). After deposition of the $Chol_{30mN/m}$ monolayer (Fig. 9c) the ribbed structure disappears and surface morphology demonstrates domain-like shape. Due to relatively high roughness of PEEKair surface the obtained roughness value equal to $S_q=5.48$ nm for $Chol_{30mN/m}$ only slightly higher than that of PEEKair can suggest similar properties of the surface which is not always consistent. Considering also morphological features provides more reliable description which facilitates comparison of the samples. In both cases the ribbed structures are clearly seen. On the other hand the forms resembling crystallites characteristic for the support are less visible if the Chol layer is present.

Deposition of the mixed Chol–CsA ($X_{CsA}=0.25$) layer leads to disappearance of ribbed structure of PEEKair as a result of filling the depressions by molecules, and the surface smoothing ($S_q=3.20$ nm, Fig. 9d). It is worth mentioning the domain structure visible on the BAM images (Fig. 6) is preserved after transferring onto PEEKair even in the case of the layer discontinuity. The most interesting structure is observed for the $X_{CsA}=0.5$ layer. Only in this case the big amorphic domains with circular shape are characteristic for each measured place of the sample (Fig. 9e). The existence of bigger domains in the floating Chol–CsA 0.5 monolayer than in the other films were observed also on the BAM images (Fig. 6). On the other hand, the increased CsA amount ($X_{CsA}=0.75$) results in the formation of ribbed surface similarly to PEEKair but without visible pseudo-crystallities. Situation is different after deposition of CsA which gives amorphic morphology of layer, similarly

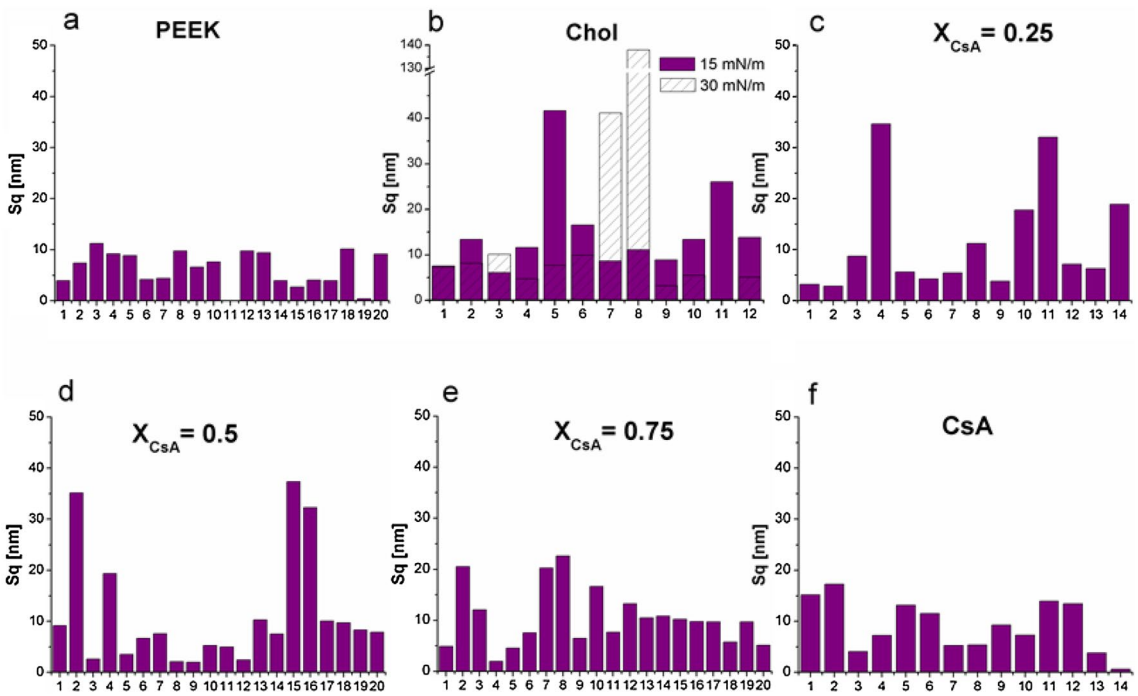

Fig. 8 Distribution of the surface roughness, S_q [nm], of: **a** PEEKair, **b** $Chol_{15mN/m}$, $Chol_{30mN/m}$, **c** $X_{CsA}=0.25$, **d** $X_{CsA}=0.5$, **e** $X_{CsA}=0.75$, **f** CsA

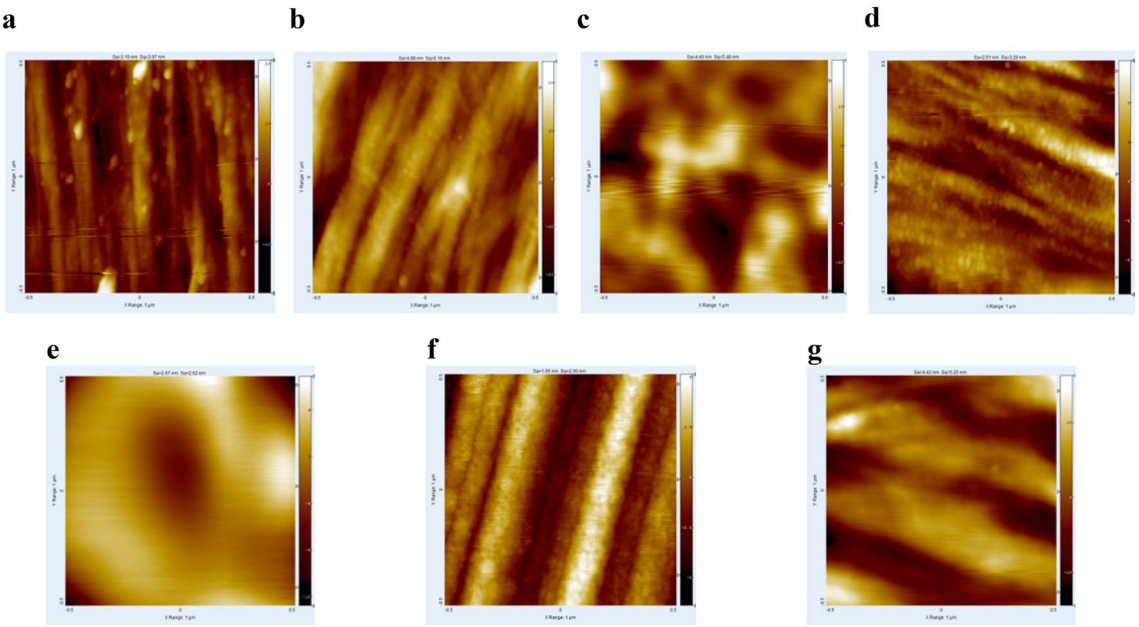

Fig. 9 AFM micrographs (1x1 μm^2) for: **a** PEEKair, S_q = 3.97 nm, **b** Chol$_{15mN/m}$, S_q = 6.16 nm, **c** Chol$_{30mN/m}$, S_q = 5.48 nm, **d** X_{CsA} = 0.25, S_q = 3.20 nm; **e** X_{CsA} = 0.5, S_q = 2.62 nm, **f** X_{CsA} = 0.75, S_q = 2.00 nm, **g** CsA, S_q = 5.25 nm

like Chol$_{30mN/m}$ but with substantially elongated domains (Fig. 9g).

We can claim that the AFM measurements provide interesting information about morphological changes between samples after the Chol–CsA deposition in different ratios. However quantitative description of roughness changes basing only on the S_q values is very uncertain. Due to high support roughness the formation of continuous monolayer coatings is hardly possible although some essential properties of the original monolayers on water subphase seem to be preserved. Moreover introduction of nanometer-sized fragmentary/imperfect monolayers on the micrometer-sized PEEKair allows forming hierarchically organized structures. They determine substantially the surface wettability that is particularly important in view of artificial bone adaptation.

3.6 Wettability of the LB films

For better characterization of the supported monolayers after the transferring process they were tested for changes in the wettability parameters and surface free energy (and its components) by the procedures described in Sect. 2.6 and 2.7, respectively.

3.6.1 Contact angles

Hydrophobic and non-polar character of the PEEK surface was predictable as for all polyarylketones (Kurtz 2012). However, the high values of contact angles obtained for polar liquids (87.5° for water and 70° for formamide) confirmed it (Fig. 10). The lowest value of advancing contact angle was obtained for non-polar diiodomethane, which was equal to 23.7°.

Low temperature and low pressure plasma activation of PEEK strongly polarizes its surface by introducing the oxygen-rich polar groups to the polymer surface (Wiącek et al. 2016a, b; Terpiłowski et al. 2018). Whereby the contact angles of polar liquids on the modified PEEK surface change significantly. Water drops revealed the average advancing contact angle of 36.4° but surprisingly formamide droplets spread onto the surface completely so the contact angle of

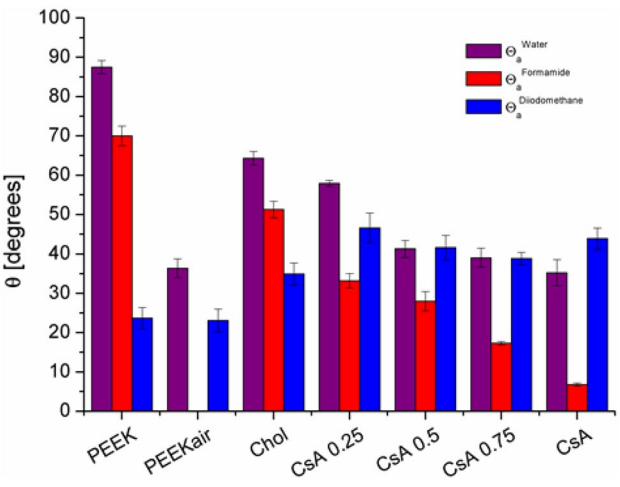

Fig. 10 Values of advancing contact angles of three test liquids on the modified PEEK surfaces

this probe liquid was assumed to be 0°. On the other hand, non-polar diiodomethane droplets were irresponsive to the PEEK surface activation and no change of contact angle was observed.

After the thin film modification the PEEK plates showed significant changes of the surface wettability compared to the PEEKair reference sample. This fact can prove the presence of monolayers embeded to the activated PEEK surface. The highest values of water contact angle are observed on the PEEKair/Chol surface (64.3°), when the Chol monolayer was transferred at 30 mN/m (Fig. 10). The influence of the amount of CsA in the Chol monolayer on the surface hydrophobicity is also manifested. The larger molar fraction of this polypeptide is used, the greater decrease of contact angle of water occurs and the PEEK surface becomes more hydrophilic. The contact angle of water drops gradually from 87.5° (for unmodified PEEK) to 64.3° (Chol), 57.9°, 41.3°, 39° for $X_{CsA} = 0.25$; 0.5; 0.75 and finally to the value 35.3° for the pure CsA. In the case of polar formamide the presence of Chol film causes a drastic increase of the advancing contact angle from 0° (PEEKair) to 51.3°. This observation can suggest that the Chol layer placed on the solid surface is condensed and does not allow the formamide molecules contact with the activated PEEK surface. For the PEEKair/Chol surface obtained at the surface pressure of 15 mN/m the average contact angle of water, formamide and diiodomethane was estimated as 48.9° ± 1.3°, 0° (total spreading) and 33.4° ± 2.1°, respectively. Those results suggest that test liquids have greater access to the activated surface than in the case of the cholesterol layer applied at higher pressure (30 mN/m). This assumption is also supported by the higher value of the cholesterol compressibility modulus observed at the surface pressure of 30 mN/m. Although as the amount of CsA in the Chol film increases, the formamide contact angles change similar to those of water (with increasing the CsA in the monolayer) and gradually decrease from 33.2° ($X_{CsA} = 0.25$) to 28°, 17.3° ($X_{CsA} = 0.5$ and $X_{CsA} = 0.75$) and finally reach a value 6.8° for pure CsA. Due to the complex structure of CsA and possible conformational changes depending on the surrounding environment it can be suggested that CsA molecule can bind with its polar moieties directly to the PEEK surface and apolar fragments up to the air. Nevertheless, it can not excluded that the other polar groups are exposed to the air being responsible for the growing surface polarity with the increasing CsA amount. On the other hand, as it was mentioned previously CsA decreases the values of Cs^{-1} parameter distinctly making the binary film loosely packed and consequently it becomes more permeable for the investigated liquids.

For the third test liquid which was non-polar diiodomethane for all deposited monolayers the increase of measured contact angles is observed compared to that on the PEEKair surface (23.1°). This increase in value is similar in all cases and is evaluated to be about 15° (Fig. 10). Similar changes can be explained based on diiodomethane interactions with other molecules which are nearly 100% dispersive and furthermore this kind of interaction does not change depending on the monolayer composition. Similar results were obtained in our previous studies (Jurak et al. 2016; Jurak and Wiącek 2017).

3.6.2 Surface free energy and its components

Much better insight into the physicochemical characteristics of the modified PEEK surface-liquid gives estimation of the surface free energy (SFE) and its components. The SFE values were calculated using the van Oss et al. approach (1989, 1990) and are presented in Fig. 11.

As it could be assumed on the basis of the previously described results of contact angles (Jurak et al. 2016; Wiącek et al. 2016a, b), PEEK air plasma activation provides the increase of γ_S^{tot} (by 12.3 mJ/m^2) compared to the unmodified PEEK surface. For unmodified PEEK the surface value of γ_S^{tot} is equal to the Lifshitz-van der Waals component (γ_s^{LW}) because $\gamma_S^{AB} = 0$. Furthermore for the PEEKair surface γ_S^{tot} (58.9 mJ/m^2) is much higher than its γ_s^{LW} component (46.8 mJ/m^2) due to the contribution of acid–base interactions ($\gamma_s^{AB} = 12.1$ mJ/m^2). PEEKair reveals $\gamma_s^+ = 1.2$ mJ/m^2 and a particularly significant increase of the electron-donor parameter $\gamma_s^- = 31.4$ mJ/m^2 is found which undoubtedly is, caused by the presence of polar groups. On the other hand, the application of the Chol monolayer on the PEEKair surface causes the decrease of γ_s^- to value 18.6 mJ/m^2. However, the presence of CsA in the Chol film results in the changes of this value. For the composition at $X_{CsA} = 0.25$ it drops to value $\gamma_s^- = 15.4$ mJ/m^2, then as a function of CsA amount

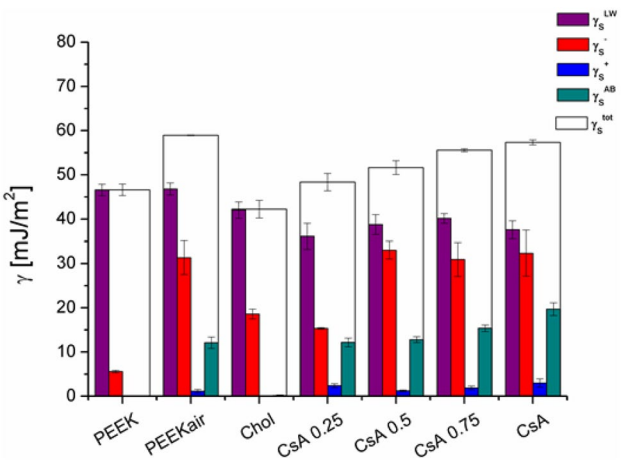

Fig. 11 Total surface free energy and its components calculated from the van Oss et al. approach for the unmodified and modified PEEK surfaces

grows rapidly up to $\gamma_s^- = 33$ and 31 mJ/m^2 for $X_{CsA} = 0.5$ and 0.75, respectively.

It should be taken into account that the presence of CsA in the binary Chol–CsA film leads to the appearance of small values of electron-acceptor (γ_s^+) as well as significant rise of the acid–base (γ_s^{AB}) component, from $\gamma_s^{AB} = 0.2$ mJ/m^2 to 12.2; 12.8; 15.4 and 19.7 mJ/m^2 for $X_{CsA} = 0.25$; 0.5; 0.75 and 1, respectively. In the case of γ_s^{tot} parameter a slight increase of its value is observed as the amount of polypeptide is higher and γ_s^{tot} reaches the maximum ($\gamma_s^{tot} = 57.3$ mJ/m^2) for the pure CsA film. Only for the Chol monolayer the value of Lifshitz-van der Waals component (γ_s^{LW}) is nearly the same as its total value $\gamma_s^{LW} = 42$ mJ/m^2 and $\gamma_s^{tot} = 42.2$ mJ/m^2, similarly to the case of unmodified PEEK.

Some correlations between the changes of γ_s^- and ΔG^{exc} can be found. The γ_s^- parameter reflects the interactions mostly by hydrogen bonding between PEEK and/or supported monolayer and test liquid molecules. Considering the mixed films one can claim that the strongest repulsive interactions between Chol and CsA appear at $X_{CsA} = 0.5$ (maximal ΔG^{exc}) (Fig. 5). At the same composition γ_s^- reaches the highest value (Fig. 11). Stronger repulsion between the Chol and CsA molecules in the monolayer can facilitate an access of water and formamide to the polar groups of the film compounds. In other words, the polar groups of Chol and CsA, weakly engaged in mutual interactions, are more readily available for polar liquids, interacting through hydrogen bridges. With the increasing amount of CsA in the monolayer the γ_s^+ interactions are getting stronger owing to probable exposition of groups capable of acidic (electron-acceptor) interactions. Finally, an increase in the acid–base interactions γ_s^{AB} is observed which proves the increased surface polarity. The BAM images (Fig. 6) at the transfer surface pressure of 15 mN/m show that monolayer morphology and structure is strongly affected by the CsA molecules even at small molar fractions. As the amount of CsA in the monolayer increases small globular domains seem to disappear and expanded areas grow. After transfer onto PEEKair the looser packed layer is more easily permeated by liquids, thus affecting the γ_s^{AB} increase. Hence one can conclude that a better insight into the interactions can be obtained by considering the components of surface free energy than its total value. Moreover, our findings prove that the LB films on PEEK preserve mostly the properties of the corresponding Langmuir monolayers in spite of using rough support.

4 Conclusions

This paper provided characteristics of the low temperature and low pressure air plasma activated PEEK surfaces coated with the cholesterol - cyclosporine A thin films as regards its roughness, wettability and changes of surface free energy. The obtained results and observations have shown a significant effect of only small amounts of cyclosporine A in the cholesterol film evidently changing the course of the π-A isotherms as well as the morphology and film thickness. After the formation of bi-component PEEK polymer coatings using the Langmuir–Blodgett technique, a substantial effect of cyclosporine A on the topography and the hydrophilic-hydrophobic nature of the modified surface was observed, and its total surface energy explicitly increased with the increasing amount of CsA in the coating. In the case of biomedical application it is important to design coatings of controlled polarity. It is difficult to determine which of the presented covers would be the best for biomedical applications due to the fact that, depending on the specific application, the hydrophobic-hydrophilic character of the surface could be very different. However, based on our results, it is known that by maneuvering the proportions of components with different polarity, a coating of a specific hydrophobic-hydrophilic character can be obtained. Therefore, cold plasma modification not only sterilizes the polymer but also allows to bind chemically or physically different substances to its surface. Although the experiments were conducted at room temperature the presented paper refers to the behaviour of molecules assuming the in vivo conditions. In summary, taking into account the theoretical properties of the obtained PEEK polymer coatings, such modifications can increase surface biocompatibility, cells adhesion or act as therapeutic substances. However, to validate the above assumptions, more experiments should be carried out.

Acknowledgements The research was carried out with the equipment purchased thanks to the financial support of the European Regional Development Fund in the framework of the Polish Innovation Economy Operational Program (contract no. POIG.02.01.00-06-024/09 Center of Functional Nanomaterials) as well as using the equipment of Center for Interdisciplinary Research, The John Paul II Catholic University, purchased owing to the financial support of the European Regional Development Fund in the framework of the Development of Eastern Poland Operational Program 2007–2013 (contract no. POPW.01.03.00-06-003/09-00).

References

Botel, F., Zimmermann, T., Sutel, M., Muller, W., Schwitalla, A.D.: Influence of different low-temperature plasma process parameters on shear bond strength between veneering composites and PEEK materials. Dent. Mater. **34**, 10246–10254 (2018)

Bhatnagar, N., Jha, S., Bhowmik, S., Gupta, G., Moon, J.B., Kim, C.: Physico-chemical characteristics of high performance polymer modified by low and atmospheric pressure plasma. Surf. Eng. Appl. Electrochem. **48**, 117–127 (2012)

Bundgaard, H., Friis, G.J.: Prodrugs of peptides 16. Isocyclosporin A as a potential prodrug of cyclosporin A. Int. J. Pharm. **82**, 85–90 (1992)

Cadena-Nava, R.D., Martin Minones, J.M., Vazques-Martinez, J., Roca, J.A., Ruiz-Garcia, J.: Direct observations of phase changes in Langmuir films of cholesterol. Rev. Mex. Fis. **52**, 32–33 (2006)

Chen, X., Lenhert, S., Hirtz, M., Lu, N., Fuchs, H., Chi, L.: Langmuir–Blodgett patterning: a bottom–up way to build mesostructures over large areas. Acc. Chem. Res. **40**, 393–401 (2007)

Comyn, J., Mascia, L., Parker, B.M.: Plasma-treatment of polyetheretherketone (PEEK) for adhesive bonding. Int. J. Adhes. Adhes. **16**, 97–104 (1996)

Costa, A.P., Xu, X., Burgess, D.J.: Langmuir balance investigation of superoxide dismutase interactions with mixed-lipid monolayers. Langmuir **28**, 10050–10056 (2012)

Davies, J.T., Rideal, E.K.: Interfacial Phenomena. Academic Press, New York (1963)

Dannes, T.J., Schwartz, J.: A nanoscale adhesion layer to promote cell attachment on PEEK. J. Am. Chem. Soc. **131**, 221–454 (2009)

Dynarowicz-Łątka, P., Kita, K.: Molecular interraction in mixed monolayers at the air/water interface. Adv. Colloid Interface Sci. **1**, 1–17 (1999)

Dynarowicz-Łątka, P., Wnętrzak, P., Makyła-Juzak, K.: Cyclosporin A in membrane lipid environment: implications for antimalarian activity of the drug—the Langmuir monolayer studies. J. Membr. Biol. **248**, 1021–1032 (2015)

Epand, R., Epand, F., McKenzie, R.: Effects of viral chemoterapeutic agents on membrane properties: studies of cyclosporin A, benzyloxylcarbonyl-D-Phe-L-Phe-Gly and amantadine. J. Biol. Chem. **262**, 1244–1249 (1987)

Favia, P., d'Agostino, P.: Plasma treatments and plasma depostion of polymers for biomedical applications. Surf. Coat. Technol. **98**, 1102–1106 (1998)

Fukuda, N., Tsuchiya, A., Sunarso, Toyta, R., Tsuru, K., Mori, Y., Ishikawa, K.: Surface plasma treatment and phosphorylation enhance the biological performance of poly(ether ether ketone). Colloids Surf. B **173**, 36–42 (2019)

Frederik, R., Raymond, M., Van Gaalen, S.M., De Gast, A., Cumhur, O.F.: Polyetheretherketone (PEEK) cages in cervical applications: a systematic review. Spine J. **15**, 1446–1460 (2015)

Gaines, G.L.: Insoluble monolayers at liquid-gas interfaces. Wiley -Interscience, New York (1966)

Gan, K., Liu, H., Jiang, L., Liu, X., Song, X., Niu, D., Chen, T., Liu, C.: Bioactivity and antibacterial effect of nitrogen plasma immersion ion implantation on polyetheretherketone. Dent. Mater. **32**, 10263–10274 (2016)

Garbassi, F., Morra, M., Occhiello, E.: Modification Techniques and Applications. Polymer Surfaces: from Physics to Technology. John Wiley and Sons, Chichester (1994)

Hawkshaw, N.J., Hardman, J.A., Haslam, I.S., Shahmalak, A., Gilhar, A., Lim, X.: Identifying novel strategies for treating human hair loss disorders: cyclosporine A suppresses the Wnt inhibitor, SFRP1, in the dermal papilla of human scalp hair follicles. PLoS Biol. **16**, 1–17 (2018)

Hubbell, J.A.: Chemical modification of polymer surfaces to improve biocompatibility. Trends Polym. Sci. **2**, 20–25 (1994)

Jurak, M., Miñones, Conde J.: Characterization of the binary mixed monolayers of α-tocopherol with phospholipids at air-water interface. Biochim. Biophys. Acta Biomembr. **11**, 2410–2418 (2013)

Jurak, M., Wiącek, A.E.: Wettability of hybrid chitosan/phospholipid coatings. Prog. Chem. Appl. Chitin Deriv. **22**, 66–76 (2017)

Jurak, M., Wiącek, A.E., Terpiłowski, K.: Properties of PEEK-supported films of biological substances prepared by the Langmuir–Blodgett technique. Colloids Surf. A **510**, 263–274 (2016)

Kantlehner, M., Schaffner, P., Finsinger, D., Meyer, J., Jonczyk, A., Diefenbach, B.: Surface coating with cyclic RGD peptides stimulates osteoblast adhesion and proliferation as well as bone formation. ChemBioChem **1**, 107–114 (2000)

Kurtz, S.: PEEK Biomaterials Handbook, 1st edn. Elsevier Science and Technology, Kindlington (2012)

Leslie, M.: Do lipid rafts exist? Science **334**, 1046–1047 (2011)

Loosli, H.R., Kessler, H., Oschkinat, H., Weber, H.P., Petcher, T.: Peptide conformations. Part 31. the conformation of cyclosporin A in the crystal and in solution. Helv. Chimica Acta **68**, 682–704 (1985)

Lvhua, L., Yanyan, Z., Xiong, Z.: Bioactive polyetheretherketone implant composites for hard tissue. Prog. Chem. **29**, 450–458 (2017)

Ma, R., Tang, T.: Current strategies to improve the bioactivity of PEEK. Int. J. Mol. Sci. **15**, 5426–5445 (2014)

Mahjoubi, H., Buck, E., Manimunda, P., Farivar, R., Chromik, R., Murshed, M., Cerruti, M.: Surface phosphonation enhances hydroxyapatite coating adhesion on polyetheretherketone and its osseointegration potential. Acta Biomater. **47**, 149–158 (2017)

Malcolm, B.R., Cadenhead, D.A., Danielli, J.F., Rosenberg, M.: Progress in surface and membrane science. Acad. Press **7**, 183–199 (1973)

Najeeb, S., Zafar, M.S., Khurshid, Z., Fahad, S.: Applications of polyetheretherketone (PEEK) in oral implantology and prosthodontics. J. Prosthodont. Res. **60**, 12–19 (2016)

Novotna, Z., Reznickova, A., Rimpelova, S., Vesely, M., Kolska, Z., Svorcik, V.: Tailoring of PEEK bioactivity for improved cell interaction: plasma treatment in action. RSC Adv. **5**, 41428–41436 (2015)

O'Learyl, T., Ross, P., Lieber, M., Levin, I.: Effects of cyclosporine A on biomembranes: vibrational spectroscopic, calorimetric and hemolysis studies. Biophys. J. **49**, 795–801 (1986)

Ohvo-Rekilä, H., Ramsted, B., Leppimaki, P., Slotte, J.P.: Cholesterol interactions with phospholipids in membranes. Prog. Lipid Res. **41**, 66–69 (2002)

Przykaza, K., Woźniak, K., Jurak, M., Wiącek, A.E.: Wetting properties of polyetheretherketone plasma activated and biocoated surfaces. Colloids Interfaces **3**, 1–14 (2019)

Rodríguez Patino, J.M., Carrera, Sánchez C., Rodríguez Niño, M.R.: Morphological and structural characteristics of monoglyceride monolayers at the air-water interface observed by Brewster angle microscopy. Langmuir **15**, 2484–2492 (1999)

Rui, M., Lin, F., Zhongkuan, L., Luqian, W., Shenhua, S., Ruisheng, Z., Hongyan, S., Huide, F.: Mechanical performance and in vivo bioactivity of functionally graded PEEK-HA biocomposite materials. J. Sol-Gel. Sci. Technol. **70**, 339–345 (2014)

Ryan, D., Getgood, A.: Implant alternatives for tibial osteotomies. J. Knee Surg. **30**, 426–434 (2017)

Schroeder, F., Woodford, J., Kavecansky, J., Wood, W., Joiner, C.: Cholesterol domains in biological membranes. Mol. Membr. Biol. **12**, 113–119 (1995)

Söderlund, T., Lehtonen, J.Y.A., Kinnunen, P.K.J.: Interactions of Cyclosporin A with phospholipid membranes: effect of cholesterol. Mol. Pharmacol. **55**, 32–38 (1999)

Terpiłowski, K., Jurak, M., Wiącek, A.E.: Influence of nitrogen plasma treatment on the wettability of polyetheretherketone and deposited chitosan layers. Adv. Polym. Technol. **37**, 1557–1569 (2018)

Van Oss, C.J., Chaudhury, M.K., Good, R.J.: Interfacial Lifshitz-van der Waals and polar interactions in macroscopic systems. Chem. Rev. **88**, 927–941 (1990)

Van Oss, C.J., Ju, L., Chaudhury, M.K., Good, R.J.: Estimation of the polar parameters of the surface tension of liquids by contact angle measurements on gels. J. Colloid Interface Sci. **128**, 313–319 (1989)

Weis, R., McConell, H.: Cholesterol stabilizes the crystal-liquid interface in phospholipid monolayers. J. Phys. Chem. **89**, 4453–4459 (1985)

Wiącek, A.E., Terpiłowski, K., Jurak, M., Worzakowska, M.: Low-temperature air plasma modification of chitosan-coated PEEK. Polym. Test. **50**, 325–334 (2016a)

Wiącek, A.E., Terpiłowski, K., Jurak, M., Worzakowska, M.: Effect of low-temperature plasma on chitosan-coated PEEK polymer characteristics. Eur. Polym. J. **78**, 1–13 (2016b)

Wiedmann, T., Trouard, T., Shekar, S., Polikandritou, M., Rahman, Y.: Interaction of cyclosporin A with dipalmitoylphosphatidylcholine. Biochim. Biophys. Acta **1023**, 12–18 (1990)

Winsel, K., Hönig, D., Lunkenheimer, K., Geggel, K., Witt, C.: Quantitative Brewster angle microscopy of the surface film of human broncho-alveolar lavage fluid. Eur. Biophys. J. **32**, 544–552 (2003)

Wnętrzak, A., Makyła-Juzak, K., Chachaj-Brekiesz, A., Lipiec, E., Romeu, N.V., Dynarowicz-Łątka, P.: Cyclosporin A distribution in cholesterol-sphingomyelin artificial membranes modeled as Langmuir monolayers. Colloids Surf. B **166**, 286–294 (2018)

Zhang, S., Awaja, F., Natalie, J., McKenzie, D., Ruys, A.: Autohesion of plasma treated semi-crystalline PEEK: comparative study of argon, nitrogen and oxygen treatments. Colloids Surf. A **374**, 88–95 (2011)